

Article

# Low-Cost Activated Carbon for Petroleum Products Clean-Up

Ramonna I. Kosheleva <sup>\*</sup>, George Z. Kyzas , Nikolaos C. Kokkinos  and Athanasios C. Mitropoulos

Department of Chemistry, International Hellenic University, St. Lucas, 65404 Kavala, Greece; kyzas@chem.ihu.gr (G.Z.K.); nck@chem.ihu.gr (N.C.K.); amitrop@chem.ihu.gr (A.C.M.)

\* Correspondence: rkosheleva@chem.ihu.gr; Tel.: +30-2510462247

**Abstract:** Petroleum products are hazardous both for humans and nature. Diesel oil is one of the main contaminants of land but also of sea, during its transportation. Currently, there are many different clean-up techniques for petroleum products. One of the most common is adsorption by adsorbent materials. Although adsorption is an eco-friendly and cost-effective approach, it lacks efficiency. The present study investigates the performance of low-cost activated carbon, derived from potato peels and activated under different temperature conditions, from 350 °C to 800 °C. The yield of activated carbon decreases with the increase in the carbonization temperature. However, the sample prepared at 600 °C shows an oil sorption capacity of 72 g/g, which is the highest of all samples. Nitrogen adsorption characterization reveals that this specific sample has the highest specific surface (SSA) area of 1052 m<sup>2</sup>/g and total a pore volume of 2.959 cm<sup>3</sup>/g, corresponding to a 94% and 77% increase compared to the sample prepared at 350 °C. Oil sorption kinetics experiments show that, for all samples, the maximum uptake is reached after 1h. Oil uptake was also investigated under realistic conditions by introducing the best performance activated carbon to an oil/seawater system, and the outcome does not show a significant decrease in the oil sorption. The outcomes of this study indicate that low-cost adsorbents from agricultural by-products have strong potential as an oil spill response technique.

**Keywords:** oil spill; low-cost activated carbon; sorption kinetics



**Citation:** Kosheleva, R.I.; Kyzas, G.Z.; Kokkinos, N.C.; Mitropoulos, A.C. Low-Cost Activated Carbon for Petroleum Products Clean-Up. *Processes* **2022**, *10*, 314. <https://doi.org/10.3390/pr10020314>

Academic Editor: David W. Mazzyck

Received: 1 December 2021

Accepted: 2 February 2022

Published: 6 February 2022

**Publisher's Note:** MDPI stays neutral with regard to jurisdictional claims in published maps and institutional affiliations.



**Copyright:** © 2022 by the authors. Licensee MDPI, Basel, Switzerland. This article is an open access article distributed under the terms and conditions of the Creative Commons Attribution (CC BY) license (<https://creativecommons.org/licenses/by/4.0/>).

## 1. Introduction

Petroleum hydrocarbon is a complex pollutant of both land and marine environments [1]. Petroleum products, such as diesel, are obtained during crude oil distillation and are made up of low molecular weight alkanes and polycyclic aromatic hydrocarbons [2]. The hydrocarbon composition of diesel fuel makes it toxic to the environment and its widespread application in human activities makes it one of the most hazardous hydrocarbon pollutants. In large quantities in water, due to its hydrophobicity, diesel forms a layer on the water surface, and it becomes easy to remove. However, in marine environments, due to wind and currents, petroleum products evaporate, spread and sediment, according to its properties [3]. If the spill response is not implemented on time, small quantities of the diesel will form an emulsion [4] with the water and more elaborate removal methods will need to be applied.

Remediation of water contaminated by petroleum hydrocarbons can be performed by a number of methods, categorized as physical or chemical [5] ones. Chemical methods include dispersants (essentially a surfactant spreading on the oil spill [6]), chemical oxidation such as the Fenton process [7], etc. Although the implemented methods showcase good performance, most of the time, they are energy consuming and not cost-effective approaches [8].

Among the physical methods, spill adsorption is considered one of the most cost effective and eco-friendly cleaning techniques [9]. However, there are some restrictions regarding its performance, such as its low sorption capacity, which in turn is characterized mainly as hydrophilic. A solution in this direction is the improvement of such materials

by surface modification. Activated carbon can be modified to gain magnetic properties for easier collection after the clean-up process [10]. Another example is to enhance its hydrophobicity by acidic additives [11].

The drawbacks of such modifications include more laborious synthesis processes and an increase in the total cost. Another important criterion in the total cost equation is the origin of activated carbon precursors. Although the most popular and commercially available activated carbons are derived from raw materials such as coconut shells [12] and rice husks [13], it is not the optimal solution for large-scale activated carbon production in the European region; such raw materials have to be imported, and thus the cost will be increased. This local abundance can be eliminated by replacement with a “universal” precursor such as food waste. Specifically, everyday life by-products, for example vegetable and fruit peels [14], tend to gain attention as a good alternative.

To this end, the present study investigates the performance of activated carbon derived from potato peels, which are prepared under different activation temperature conditions, for oil adsorption. Examination of sorbents’ performance for the specific application is restricted by the simulation of the real environment, where in addition to temperature and aqueous phase composition, there are natural impact factors such as currents and the wildlife of the area. The main criterion of the performance is the sorption capacity of the material, while kinetics play a significant role as well. The experimental design aims to find the optimal synthesis conditions that result in a high SSA (specific surface area) and total pore volume ( $V_{\text{tot}}$ ) activated carbon and then examine its performance for oil spill cleaning applications. Material characterization by  $N_2$  adsorption measurements indicates the sample with the best structural properties, while SEM (scanning electron microscopy) visualizes the selected sample. Activated carbon yield, oil sorption kinetics and material reusability were examined for material performance evaluation. For reasons of comparison, realistic conditions were simulated too.

## 2. Materials and Methods

### 2.1. Materials

For the experiment, commercially available oil (diesel) was used as the petroleum product, while the activated carbon (AC) sorbent was synthesized in the lab. To examine sorption performance closer to the real environment, seawater from the region was used after filtration with filter paper in order to avoid any solid matter.

#### 2.1.1. Activated Carbon Synthesis

For AC synthesis, waste potato peels collected from local restaurants were used. Primarily, the potato peels were cleaned of dust and other impurities by washing with distilled water. Next, the moisture was reduced by drying for 24 h in an oven at 393 K. The resulting biomass was ground and sieved in order to obtain a specific size and a more homogeneous shape.

The synthesis process was described analytically in a previous work [15]. Briefly, chemical activation of dry biomass was achieved with phosphoric acid ( $H_3PO_4$ ). An amount of 10 g of dry potato peel precursor was impregnated with 125 mL of  $H_3PO_4$  (75%  $w/w$ ) at room temperature and kept under stirring for 24 h. The impregnated biomass was dried in a sand bath at high temperature in order to remove residual water and then oven-dried for 24 h at 100 °C.

A weighed amount of the dried impregnated samples was placed in a furnace and heated from 350 to 800 °C (with 50 °C interval) activation temperatures. The treatments were carried out with a nitrogen flow (99.999% pure) of 30 STP  $cm^3/min$ ; the latter was kept at the same rate during heating and cooling, and at a constant heating rate of 10 K/min. The treatment at the activation temperature lasted 2 h, and after cooling, the solid residues were washed in a Soxhlet apparatus for 24 h until neutral pH and then with ethanol. The resulted activated carbons were dried at 100 °C for 24 h.

The code name of the prepared samples includes an ACp prefix (activated carbon from potato peels) followed by a number corresponding to each activation temperature; for example, ACp-450 is for a sample activated at 450 °C. The effect of the carbonization time on the yield followed the synthesis process.

### 2.1.2. Material Characterization

All the prepared samples were characterized regarding their structure and porous properties by isothermal adsorption measurements. Surface area according to the BET equation was obtained at 77 K by a N<sub>2</sub> porosimeter (Quantachrome, NOVA<sup>®</sup> e-Series Surface Area Analyzer, Boynton Beach, Florida, U.S.). Prior to the measurement, each sample was properly prepared in the apparatus degasser station, where degassing for 8 h at 250 °C was performed.

Scanning electron microscopy (SEM) was performed (JEOL, JSM-6390LV, Akishima, Tokyo, Japan) for morphological characterization of the prepared samples (ACp-350 and ACp-600).

## 2.2. Experimental Procedure

### 2.2.1. Activated Carbon Yield

The resulting activated carbon yield for each activation temperature was calculated by weighing the biomass before the synthesis process and the amount of the resulting material.

### 2.2.2. Sorption Kinetics

For the sorption kinetics experiments, 100 mL of the oil was poured into a conical flask. An amount of 0.5 g of the prepared AC sample was enclosed in a paper bag and weighted prior to the run and then immersed in the flask. Each run was repeated four times at 20 °C, controlled by a water bath. The contact times selected were 10, 20, 30, 40, 50, 60, 70, 80, 90, 100, 1300 and 1450 min for all prepared samples (from ACp-300 to ACp-800). After each run, samples were left to air-dry for 24 h. The amount of oil removed was the mass difference of the AC samples prior to and after each run, given by:

$$\text{Oil}_{\text{sorption}} = \frac{m_{\text{af}} - m_{\text{ai}}}{m_{\text{ai}}} \quad (1)$$

where  $m_{\text{ai}}$  and  $m_{\text{af}}$  are the initial and final masses of the adsorbent, respectively. Oil capacity in g/g of the adsorbent is given by further dividing by the total weight of the prepared sample bag.

### 2.2.3. Real Environment Simulation

In order to investigate sorbent uptake properties in the presence of salinity, an experiment was conducted by introducing the sample bag (ACp-600 staple) into a conical flask containing the same amount of seawater and oil (50 mL each). Specifically, oil was poured carefully into the flask, forming a layer on the water surface. The sample bag was hung so to have contact only with the layer of diesel. Sample bags were weighted before and after each run as in the previous experiment. The uptake was calculated once more from Equation (1).

## 3. Results and Discussion

To better evaluate the experimental results, a step-by-step procedure was followed. At first, the characterization of the materials was achieved by using BET analysis regarding structural properties with SEM for sample morphology. Then, the activated samples were adsorptively evaluated by varying the experimental conditions of the process.

### 3.1. Material Characterization

#### 3.1.1. Activated Carbon Yield

To study the effect of carbonization of potato peels on oil adsorption, the yield of the prepared activated carbon samples (ACp-350, ACp-400, ACp-450, ACp-500, ACp-550, ACp-600, ACp-650, ACp-700, ACp-750 and ACp-800) clearly shows a decrease with increasing carbonization temperature. In particular, the sample ACp-350 presented 56% yield, while the ACp-800 sample had a yield of 43% from the initial amount. Figure 1 presents this gradual decrease.

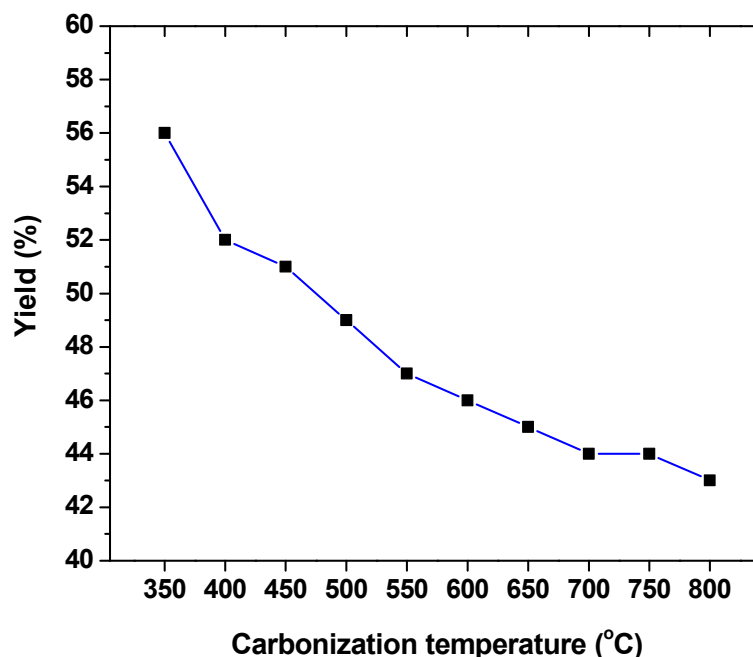
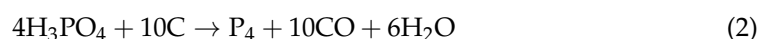


**Figure 1.** Effect of the carbonization temperature of the prepared samples on their yield.

This decrease (by increasing the carbonization temperature) is normal and was observed in other published works [12,16,17], especially in the case of other peels (from vegetables, fruits) [18,19] or polymeric sources [17]. So, it can be concluded that the source plays a key role on the final yield of any AC sample. The major explanation of the above behavior is thermal degradation; in particular, the degradation because of the phosphor-carbonaceous species and the respective reduction of the phosphates present to elemental phosphorus. The latter caused the formation of volatile phosphorous compounds,  $P_4O_{10}$  (phosphorus(V) oxide) and P (elemental form). Moreover, phosphorus (elemental) will also be a product of the activation procedure (by using  $H_3PO_4$ ) of phosphorus-containing phenol resins. The volatile phosphorus compounds may be formed according to the following reactions:



#### 3.1.2. BET Analysis

To further characterize the samples prepared, the porosity of the samples was analyzed by measurements of  $N_2$  adsorption. So, the major textural surface characteristics were observed. The SSA (specific surface area) and other porosity parameters were calculated for all the prepared samples and are given in Table 1.

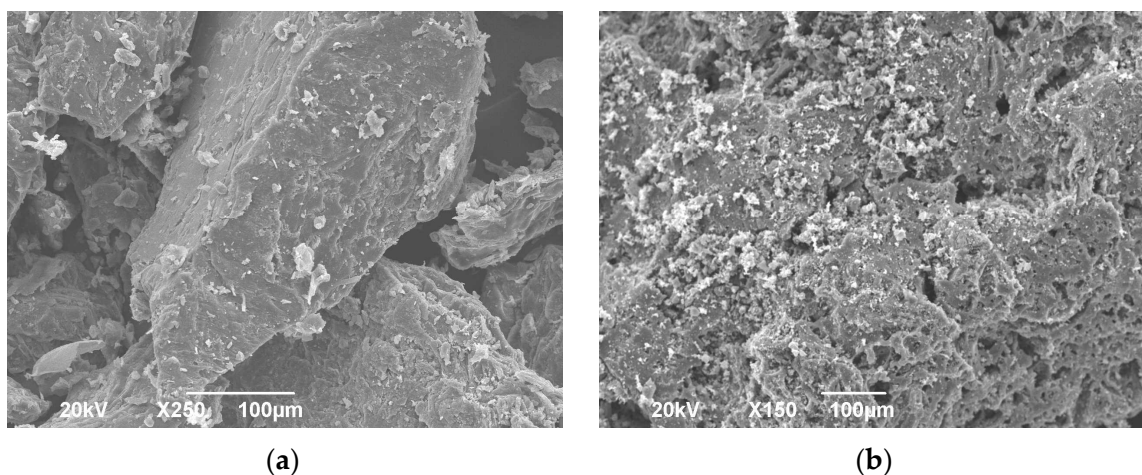
**Table 1.** Parameters of the pore structure calculated from nitrogen adsorption isotherms.

Adsorbent	Specific Surface	Micropore	Mesopore	Total Pore
	Area m <sup>2</sup> /g	Volume cm <sup>3</sup> /g	Volume cm <sup>3</sup> /g	Volume cm <sup>3</sup> /g
ACp-350	542	0.081	0.362	0.669
ACp-400	899	0.092	0.357	0.737
ACp-450	942	0.087	0.348	0.994
ACp-500	998	0.071	0.342	1.582
ACp-550	1025	0.068	0.339	2.321
ACp-600	1052	0.052	0.333	2.959
ACp-650	1032	0.031	0.251	2.733
ACp-700	221	0.030	0.125	0.586
ACp-750	112	0.021	0.089	0.342
ACp-800	5	0.002	0.003	0.005

The surface area of ACp-350 (542 m<sup>2</sup>/g) is smaller by 66% than that of ACp-400 (899 m<sup>2</sup>/g). However, by increasing the carbonization temperature from 350 to 600 °C, a gradual increase in SSA was clearly observed. As can be seen, there is a crucial carbonization temperature range (from 550 to 650 °C) over which the SSA decreases. This is normal in terms of activated carbon chemistry and can be attributed to damage (and in some cases further collapse) of the sample structure. In the case of oil adsorption, the major factor is the volume of the samples in line with the SSA. So, the above characteristics can be used to select the most appropriate sample for the oil experiments.

### 3.1.3. SEM Micrographs

Scanning Electron Microscopy was used in order to visualize the surface morphology of the ACp-600 (best oil sorption performance) and ACp-800 (lowest oil sorption performance) samples. Figure 2 presents the surface morphology of both samples. For ACp-800, the SEM micrograph shows layer-formed AC particles with dispersed agglomerates on the surface estimated to be due to the synthesis process and possible formation of carbon crystals [18], but no pore openings are visible.

**Figure 2.** SEM micrographs; (a) ACp-800 and (b) ACp-600.

The latter fact supports the N<sub>2</sub> adsorption measurement results, where the specific sample showcased the minimum SSA and V<sub>tot</sub> of all samples. On the contrary, ACp-600 in Figure 2b, shows pores with good distribution on the surface of the sample, while it preserves its layered formation.

### 3.2. Sorption Evaluation

#### 3.2.1. Sorption Capacity

The sorption evaluation is the major parameter that affects the process given that it is very important in real conditions (i.e., oil spills) to use “fast” sorbents with high capacity. Figure 3 shows the sorption capacity expressed in grams of oil per gram of ACp for the different samples prepared (different carbonization temperatures during synthesis).

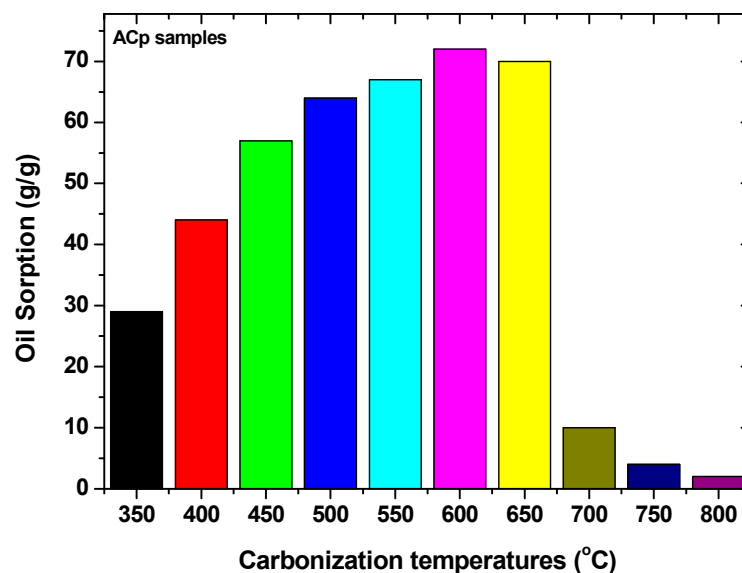
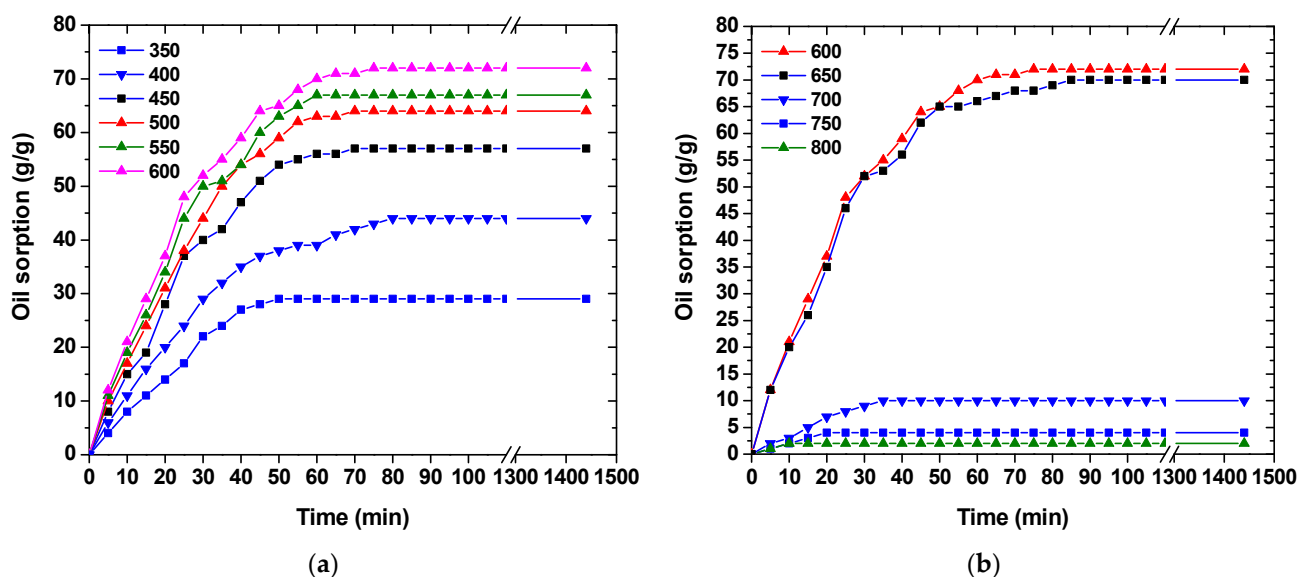


Figure 3. Effect of carbonization temperature on oil sorption.

The most efficient ACp sample prepared is that prepared at 600 °C (carbonization). It seems that by increasing the temperature of carbonization, the SSA and  $V_{\text{tot}}$  increases, which consequently causes the oil sorption to increase. In particular, the oil sorption capacity increased from ACp-350 to ACp-600 by 148%. Then, a slight decrease was observed for the sample ACp-650 (2.5%—from 72 to 70 g/g). However, a drastic reduction of 86% was clear from the 650 to 700 °C samples. This intense decrease can be attributed to the collapse of the material which “deactivated” the sorptive sites and the so-called “structure” of the material; the latter can be confirmed from Table 1. In general, at first the oil molecules will be diffused onto the material’s surface, so the oil molecules then become entrapped in the material because of the capillarity (capillary effects). The result is the agglomeration of the oil droplets in the porous network. It should be noted that the majority of the composition of oil is non-polar hydrocarbons; therefore, their sorption can be due to physical non-covalent interactions (van der Waals forces).

#### 3.2.2. Sorption Kinetics

Figure 4 shows the affinity of AC samples to oil with regard to time. It should be noted that the experimental points are the average of four experimental measurements. The first finding, regarding the samples prepared with carbonization temperatures from 350 to 600 °C, is the similar kinetic trend and the obvious splitting of the kinetic areas. All samples from 5 to 35 min showed a strong increase in the oil sorption. This is absolutely normal and can be explained by considering the AC surface chemistry. When the oil comes in contact with the material, the molecules try to find the appropriate active site to be adsorbed. This phenomenon is very intense in the first stages of contact because the material is “empty”. By increasing the contact time, the first oil molecules that have come in contact with the AC samples were already adsorbed, so the available active sites are fewer and the oil molecules cannot easily find sites.



**Figure 4.** Effect of contact time on oil sorption capacity. (a) ACp-350, ACp-400, ACp-450, ACp-500, ACp-550, ACp-600; (b) ACp-600, ACp-650, ACp-700, ACp-750, ACp-800.

After a fixed time (as we can see after 1 h), all active sites are filled with oil and the residual ones are in the solution (liquid phase) and cannot be adsorbed. So, the three kinetic regions of (i) sharp, (ii) gradual, and (iii) equilibrium can follow the widely known theory of sorption kinetics. The aforementioned behavior is the same for all materials with some very slight changes because all of them are of the same type (activated carbons from the same source).

On the other hand, the sorption capacity is different for the prepared AC samples, but they follow a fully explainable order. In particular, the material with the highest capacity (72 g/g) has the highest SSA (ACp-600, 1052 m<sup>2</sup>/g) and  $V_{\text{tot}}$ . (2.959 cm<sup>3</sup>/g). This indicates that the increase in carbonization temperature from 350 to 600 °C had positive effects on the textural characteristics of the AC samples and consequently on their sorption capacity. The more SSA and  $V_{\text{tot}}$  the material presents, the higher capacity they have.

However, after the crucial value of 600 °C, the further carbonization affected the sorption negatively because the structure of the samples was damaged. This behavior seems to be exponential in the cases of 700–800 °C.

### 3.2.3. Real Environment Simulation

The selected sample for this case was again ACp-600, while contact times were 5, 10, 20, 30, 45, 60, 90 and 120 min. Figure 5 shows a comparative plot of oil sorption capacity of ACp-600 in oil and oil/seawater systems (Figure 5a). In Figure 5b, a comparison of ACp-600 sorption capacity in seawater with ACp-700 in oil is presented in order to quantitatively evaluate oil sorption. As can be observed, the oil uptake is affected by the system's complexity with the presence of seawater, while time dependence is not so pronounced. On the other hand, the sorption process seems to have a sharper increase in the first 15 min compared to that of the oil system.

The sorption capacity of ACp-600 decreases by 77% in the oil/seawater system. This decrease can be attributed to oil solubility, which increases as salinity increases [19]. Despite the lower total performance, ACp-600 in seawater preserves its superiority compared to samples prepared at higher carbonization temperatures. In fact, as can be seen in Figure 5b, ACp-600 in seawater has faster, sharper and 39% more oil uptake than ACp-700. The latter fact supports the estimation that initial oil sorption capacity of ACp-600 is depressed due to higher oil solubility and pore occupation by seawater salts.

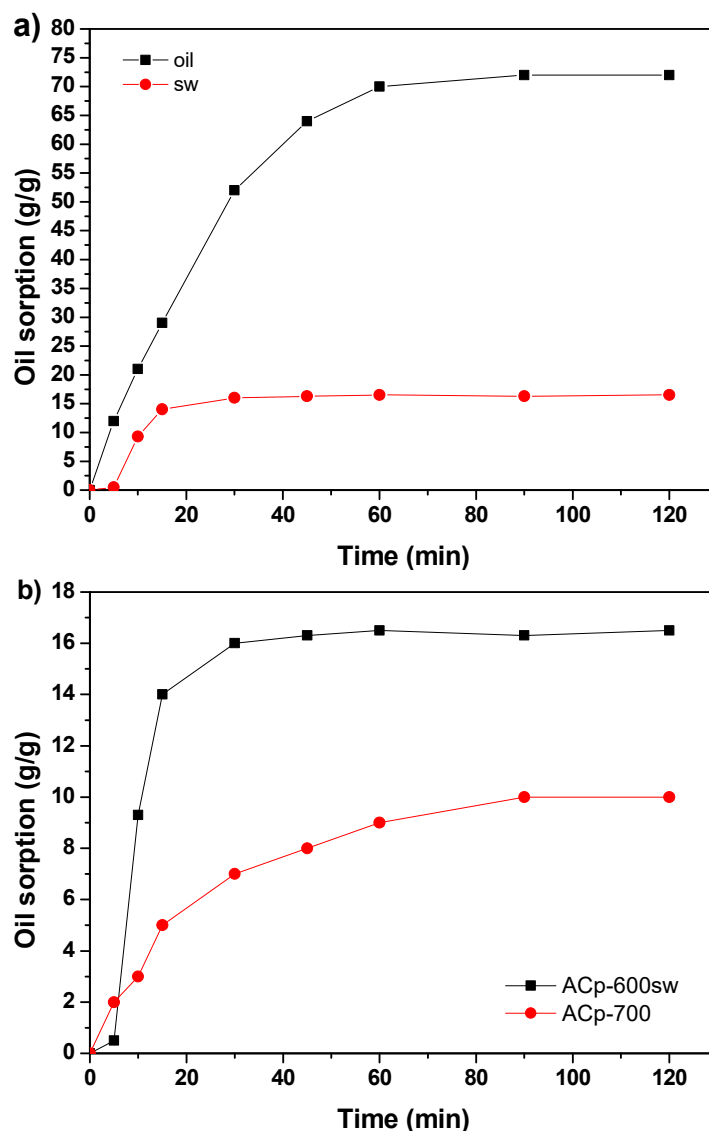


**Figure 5.** Comparative oil sorption capacity at 20 °C; (a) ACp-600 in oil and ACp-600 in oil/seawater system (ACp-600sw), (b) ACp-600sw and ACp-700 in oil system.

In order to validate the experimental results, oil sorption kinetic models were performed. The selected models were the linear driving force (LDF) model and the fractal-like linear driving force (FL-LDF) model. Figure 6 shows experimental results fitted with the two selected oil sorption kinetic models. Both models are similar, with LDF being more simplistic, presenting a linear relationship of sorption with time.

The fractal-like linear driving force includes oil observed (apparent) diffusion coefficient alteration, with time, due to a non-uniform size distribution of the material. Parameters of both models are summarized in Table 2. For the LDF model, the equation applied is:

$$m_t = m_{\max}[1 - \exp(-\beta t)] \quad (5)$$

where  $m_t$  and  $m_{\max}$  are the amount of oil absorbed after each contact time and the maximum oil absorption capacity of the pores, respectively, designated as g/g of the adsorbent. Variable  $\beta$  is the mass transfer coefficient related linearly to the apparent diffusion coefficient of oil into the pores.

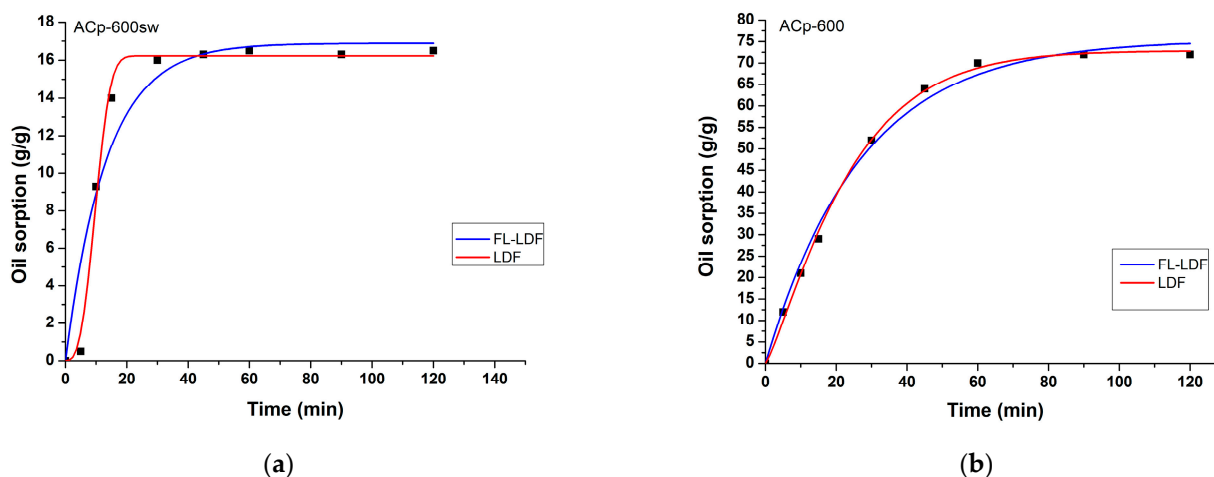


**Figure 6.** Comparison of experimental data with oil sorption kinetic models, Fractal-Like Linear Driving Force (FL-LDF) and Linear Driving Force (LDF, bottom for. (a) ACp-600 in the oil/seawater system (b) ACp-600 in oil.

**Table 2.** Parameters of the FL-LDF and LDF model for ACp-600 in oil and oil/seawater systems.

System	Model	$m_{\max}$ (g/g)	$\beta$ (s <sup>-1</sup> )	$\alpha$	$D'$	$R^2$
ACp-600	FL-LDF	72.87	-	0.49	0.021	0.998
	LDF	75.43	0.037	-	-	0.993
ACp-600sw	FL-LDF	16.23	-	0.9	0.009	0.991
	LDF	16.89	0.075	-	-	0.907

The fractal-like linear driving force is derived from [20]:

$$m_t = m_{\max}[1 - \exp(-D't^\alpha)] \quad (6)$$

where  $D'$  is the progressive, so-called observed diffusion coefficient and  $\alpha$ ,  $0 < \alpha \leq 1$ , is a constant indicating the uniformity of pore size; an approximation to 1 means a more homogenous size distribution.

In both cases, the best fitting is presented by the FL-LDF model. Model fitting provides more information about the complexity of the oil/seawater system. Specifically, parameter  $D'$ , which corresponds to the diffusion coefficient, decreases in the case of the ACp-600sw system due to increased viscosity of the oil because of the salinity [21]. On the other hand, constant  $\alpha$ , which is determined by the uniformity of porous size, increases, thus leading to the estimation that the  $\alpha$  value is increased due to the fact that dissolved salts from the seawater “blocks” some of the pores, resulting in a false size homogeneity.

### 3.3. Reuse

A very important factor to evaluate is the ability of the sorbent to be reused [22]. In Figure 7, the reuse ability of the ACp-600 is presented. The material was selected for this test because it presented the highest sorption capacity (see previous section). As can be observed, the material lost only 5% after 40 sequential reuse sorption–desorption cycles. This makes this AC sample very promising for oil-spill clean-up technology.

The prepared material shows great stability while possessing high oil uptake capacity, attributed to the porous structure of the adsorbent obtained during the synthesis process. It is believed that the specific material could be combined with mechanical assistance, such as rotation. Rotation of the adsorbent in a drum for oil spill response would increase the surface contact of oil with the material. In fact, experimental results of gas adsorption under rotation [23], as well as preliminary results of this work’s continuation, showcase

strong indications to this end. Additionally, regarding the material's hydrophobic nature, rotation would provide the desired potential to uptake oil rather than the underlying water.

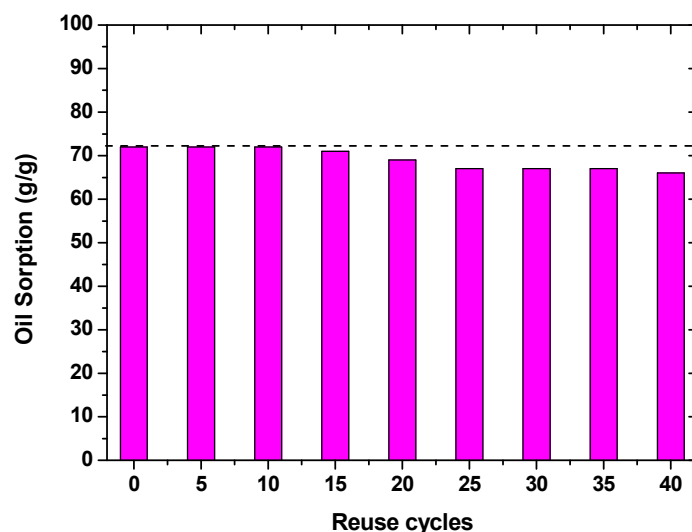


Figure 7. Reuse ability of ACp-600 after up to 40 cycles of use.

#### 4. Conclusions

Petroleum products are toxic, complex hydrocarbon compounds that when spilled, either in oceans or on land, cause severe issues for ecology, including humans. There are a number of oil-spill response and clean-up techniques, some of them efficient but not cost-effective and vice versa. One eco-friendly and cost-effective approach is oil sorption onto adsorbent materials. Such materials should present (i) efficiency, (ii) reusability and (iii) availability regarding raw materials. This work investigates a low-cost activated carbon derived from potato peels with good potential for oil spills, and in general petroleum products, remediation in water. The results of this specific study reveal that carbonization temperature plays a crucial role in the pore structure of the final material, showing a maximum increase in SSA ( $1052 \text{ m}^2/\text{g}$ ) at  $600 \text{ }^\circ\text{C}$  followed by an almost exponential decrease at the higher temperatures, with a 94% increase from the low carbonization temperature ( $350^\circ\text{C}$ ) sample. Regarding the total volume, another critical property, the same sample presents a value of  $2.959 \text{ cm}^3/\text{g}$ , which corresponds to a 74% higher level than the sample with the lowest total pore volume. Therefore, the specific sample presents the highest oil uptake of  $72 \text{ g/g}$ . Although the same sample performs only 1/3 of the uptake when seawater is present, its good reusability rate is promising for application in oil spill clean-up. Further research is directed towards the assistance of the oil spill adsorption assisted by mechanical means, such as rotation, that has been shown to increase the material's capacity compared to static conditions.

**Author Contributions:** Conceptualization, R.I.K.; methodology, G.Z.K.; validation, R.I.K.; formal analysis, N.C.K.; investigation, R.I.K.; writing—original draft preparation, R.I.K., N.C.K.; writing—review and editing, N.C.K., A.C.M. and G.Z.K.; project administration, A.C.M. All authors have read and agreed to the published version of the manuscript.

**Funding:** This research is co-financed by Greece and the European Union (European Social Fund-ESF) through the Operational Program «Human Resources Development, Education and Lifelong Learning 2014–2020» in the context of the project: “Adsorption capacity enhancement of activated carbon from agricultural wastes under a rotational field (spin adsorption): application for oil spills cleaning”(MIS 5048225).

**Institutional Review Board Statement:** Not applicable.

**Informed Consent Statement:** Not applicable.

**Data Availability Statement:** Not applicable.

**Conflicts of Interest:** The authors declare no conflict of interest.

## References

1. Cozzarelli, I.M.; Mckelvie, J.R.; Baehr, A.L. Volatile Hydrocarbons and Fuel Oxygenates. In *Treatise on Geochemistry*, 2nd ed.; Holland, H.D., Turekian, K.K., Eds.; Elsevier: Oxford, UK, 2013; Volume 11, pp. 439–480; ISBN 9780080983004.
2. Gad, S.C. *Diesel Fuel*; Wexler, P., Ed.; Elsevier: New York, NY, USA, 2005; pp. 19–22; ISBN 978-0-12-369400-3.
3. Gong, Y.; Zhao, X.; Cai, Z.; O'Reilly, S.E.; Hao, X.; Zhao, D. A review of oil, dispersed oil and sediment interactions in the aquatic environment: Influence on the fate, transport and remediation of oil spills. *Mar. Pollut. Bull.* **2014**, *79*, 16–33. [[CrossRef](#)] [[PubMed](#)]
4. Abdulredha, M.M.; Siti Aslina, H.; Luqman, C.A. Overview on petroleum emulsions, formation, influence and demulsification treatment techniques. *Arab. J. Chem.* **2020**, *13*, 3403–3428. [[CrossRef](#)]
5. Doshi, B.; Sillanpää, M.; Kalliola, S. A review of bio-based materials for oil spill treatment. *Water Res.* **2018**, *135*, 262–277. [[CrossRef](#)] [[PubMed](#)]
6. Murawski, S.A.; Schlüter, M.; Paris, C.B.; Aman, Z.M. *Summary of Contemporary Research on the Use of Chemical Dispersants for Deep-Sea Oil Spills BT—Scenarios and Responses to Future Deep Oil Spills: Fighting the Next War*; Murawski, S.A., Ainsworth, C.H., Gilbert, S., Hollander, D.J., Paris, C.B., Schlüter, M., Wetzel, D.L., Eds.; Springer International Publishing: Cham, Switzerland, 2020; pp. 494–512; ISBN 978-3-030-12963-7.
7. Sivagami, K.; Anand, D.; Divyapriya, G.; Nambi, I. Treatment of petroleum oil spill sludge using the combined ultrasound and Fenton oxidation process. *Ultrason. Sonochem.* **2019**, *51*, 340–349. [[CrossRef](#)] [[PubMed](#)]
8. Montewka, J.; Weckström, M.; Kujala, P. A probabilistic model estimating oil spill clean-up costs – A case study for the Gulf of Finland. *Mar. Pollut. Bull.* **2013**, *76*, 61–71. [[CrossRef](#)] [[PubMed](#)]
9. Mohammad, A.F.; Mourad, A.A.-H.I.; Galiwango, E.; Lwisa, E.G.; Al-Marzouqi, A.H.; El-Naas, M.H.; Van der Bruggen, B.; Al-Marzouqi, M.H. Effective and sustainable adsorbent materials for oil spill cleanup based on a multistage desalination process. *J. Environ. Manage.* **2021**, *299*, 113652. [[CrossRef](#)] [[PubMed](#)]
10. Nazifa, T.H.; Uddin, A.S.M.S.; Islam, R.; Hadibarata, T.; Salmiati; Aris, A. Oil Spill Remediation by Adsorption Using Two Forms of Activated Carbon in Marine Environment. In Proceedings of the 2018 International Conference on Computing, Electronics & Communications Engineering (iCCECE), Southend, UK, 16–17 August 2018; pp. 162–167.
11. Navarathna, C.M.; Bombuwala Dewage, N.; Keeton, C.; Pennisson, J.; Henderson, R.; Lashley, B.; Zhang, X.; Hassan, E.B.; Perez, F.; Mohan, D.; et al. Biochar Adsorbents with Enhanced Hydrophobicity for Oil Spill Removal. *ACS Appl. Mater. Interfaces* **2020**, *12*, 9248–9260. [[CrossRef](#)] [[PubMed](#)]
12. Liang, Q.; Liu, Y.; Chen, M.; Ma, L.; Yang, B.; Li, L.; Liu, Q. Optimized preparation of activated carbon from coconut shell and municipal sludge. *Mater. Chem. Phys.* **2020**, *241*, 122327. [[CrossRef](#)]
13. Alam, M.M.; Hossain, M.A.; Hossain, M.D.; Johir, M.A.H.; Hossen, J.; Rahman, M.S.; Zhou, J.L.; Hasan, A.T.M.; Karmakar, A.K.; Ahmed, M.B. The potentiality of rice husk-derived activated carbon: From synthesis to application. *Processes* **2020**, *8*, 203. [[CrossRef](#)]
14. Kosheleva, R.I.; Mitropoulos, A.C.; Kyzas, G.Z. Synthesis of activated carbon from food waste. *Environ. Chem. Lett.* **2019**, *17*, 429–438. [[CrossRef](#)]
15. Kyzas, G.Z.; Deliyanni, E.A.; Matis, K.A. Activated carbons produced by pyrolysis of waste potato peels: Cobalt ions removal by adsorption. *Colloids Surfaces A Physicochem. Eng. Asp.* **2016**, *490*, 74–83. [[CrossRef](#)]
16. Puziy, A.M.; Poddubnaya, O.I.; Martínez-Alonso, A.; Suárez-García, F.; Tascón, J.M.D. Surface chemistry of phosphorus-containing carbons of lignocellulosic origin. *Carbon N. Y.* **2005**, *43*, 2857–2868. [[CrossRef](#)]
17. Puziy, A.; Poddubnaya, O.; Martínez-Alonso, A.; Suarez-Garcia, F.; Tascón, J. Synthetic carbons activated with phosphoric - Acid I. Surface chemistry and ion binding properties. *Carbon N. Y.* **2002**, *40*, 1493–1505. [[CrossRef](#)]
18. Li, Z.; Kim, J.; Chaudhari, V.; Suseeladevi, M.; Campos, L. Degradation of metaldehyde in water by nanoparticle catalysts and powdered activated carbon. *Environ. Sci. Pollut. Res. Int.* **2017**, *24*, 17861–17873. [[CrossRef](#)] [[PubMed](#)]
19. Shiu, W.Y.; Bobra, M.; Bobra, A.M.; Majanen, A.; Suntio, L.; Mackay, D. The water solubility of crude oils and petroleum products. *Oil Chem. Pollut.* **1990**, *7*, 57–84. [[CrossRef](#)]
20. Khosravi, M.; Azizian, S. A new kinetic model for absorption of oil spill by porous materials. *Microporous Mesoporous Mater.* **2016**, *230*, 25–29. [[CrossRef](#)]
21. Ogolo, N.A.; Adesina, D.O.; Akinboro, G.O.; Onyekonwu, M.O. Effect of Water Salinity on Crude Oil Viscosity in Porous Media at Varying Temperatures. *SPE Niger. Annu. Int. Conf. Exhib.* **2019**, D023S010R002.
22. Qu, G.; Kou, L.; Wang, T.; Liang, D.; Hu, S. Evaluation of activated carbon fiber supported nanoscale zero-valent iron for chromium (VI) removal from groundwater in a permeable reactive column. *J. Environ. Manage.* **2017**, *201*, 378–387. [[CrossRef](#)] [[PubMed](#)]
23. Kosheleva, R.I.; Karapantsios, T.D.; Kostoglou, M.; Mitropoulos, A.C. A novel device for in situ study of gas adsorption under rotation. *Rev. Sci. Instrum.* **2021**, *92*, 45106. [[CrossRef](#)] [[PubMed](#)]